A new distance measure
using L'CO-FWHM correlation

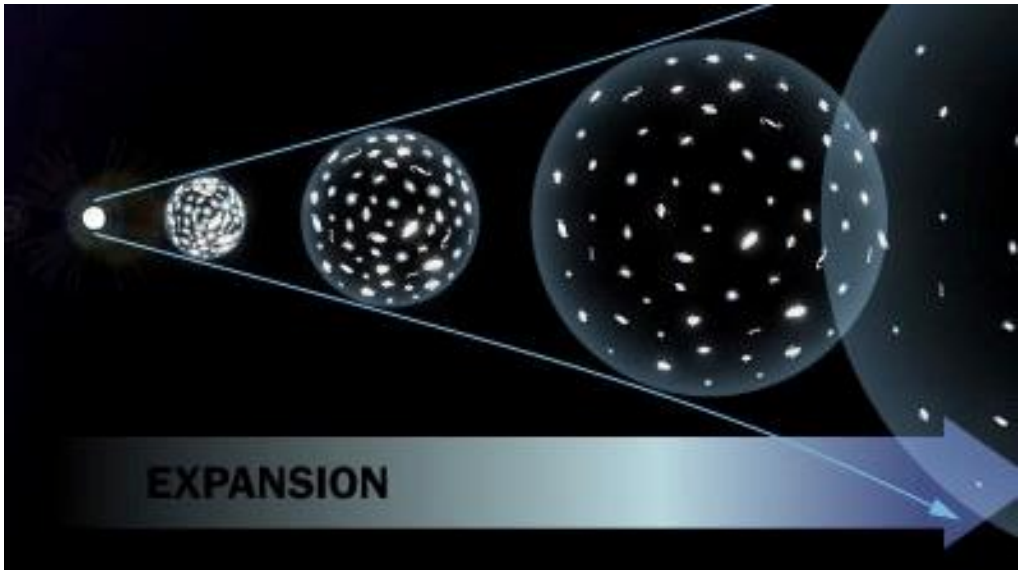

- Tomo GOTO(NTHU)
- Sune Toft (Dark Cosmology Centre)

Goto & Toft, A&A, 579 (2015) A17

Dark Energy

One of the biggest mysteries of modern astronomy/physics.

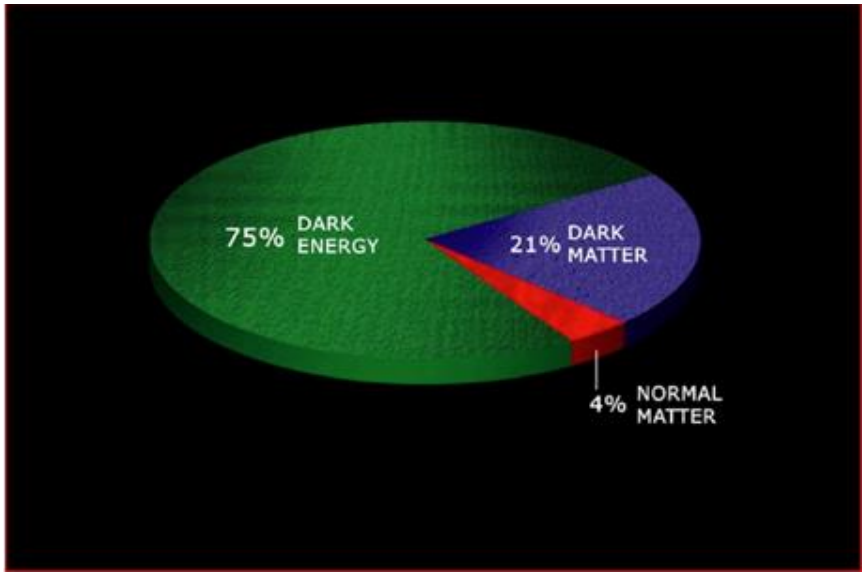

Nobel physics prize honours accelerating Universe find

By Jason Palmer
Science and technology reporter, BBC News

The three researchers' work has led to an expanding knowledge of our Universe

The next key question.
Is Dark Energy time variable?

Dark energy equation of state, w=p/ρ

$$w(z) = w_0 + w_z z/(1+z).$$

c.f. w=-1 : cosmological constant
w=1/3 : radiation

State-of-the-art

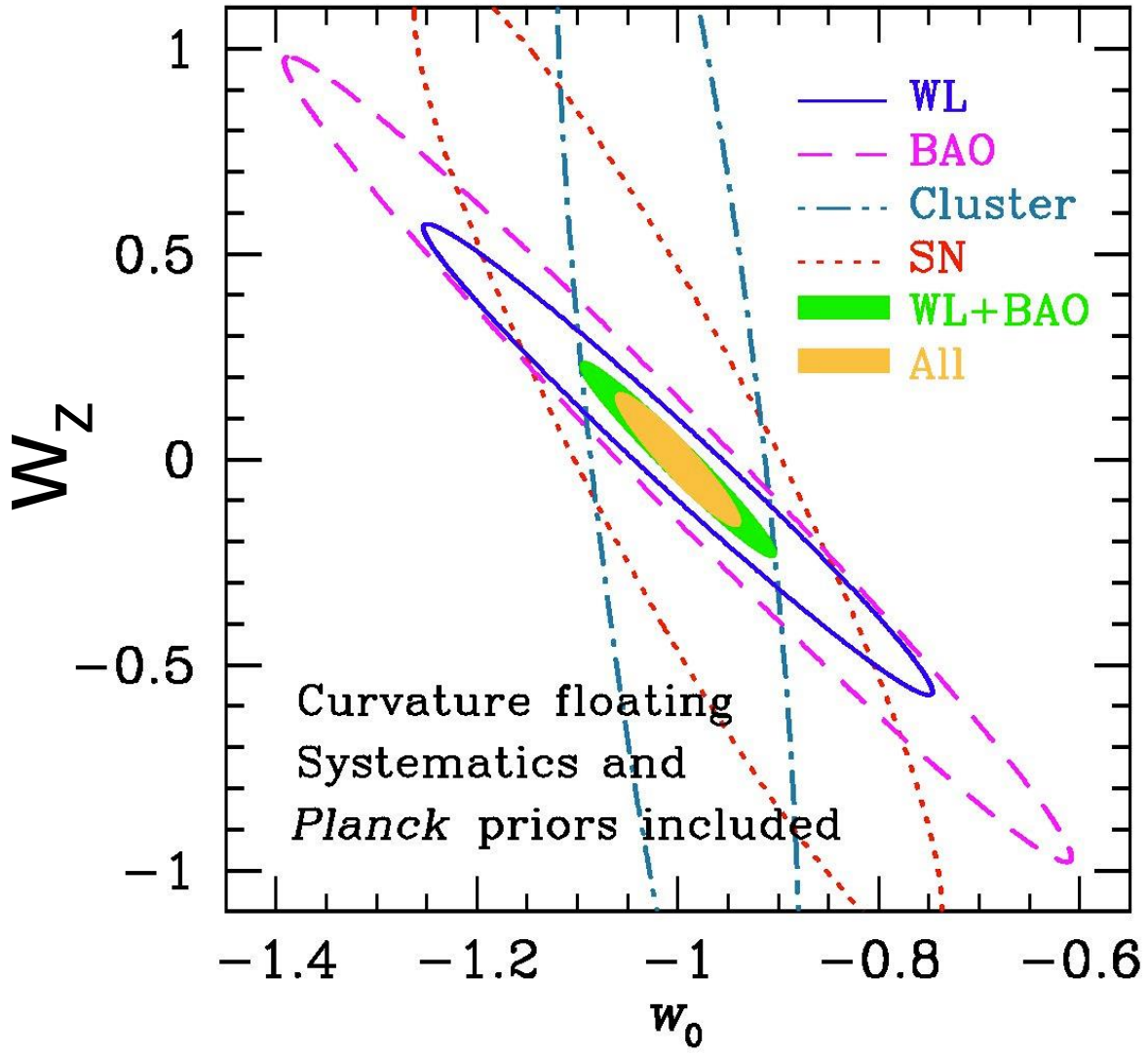

$\rho/p=w_0+w_z\ z/(1+z)$

Variability of Dark Energy

→probe at high-z

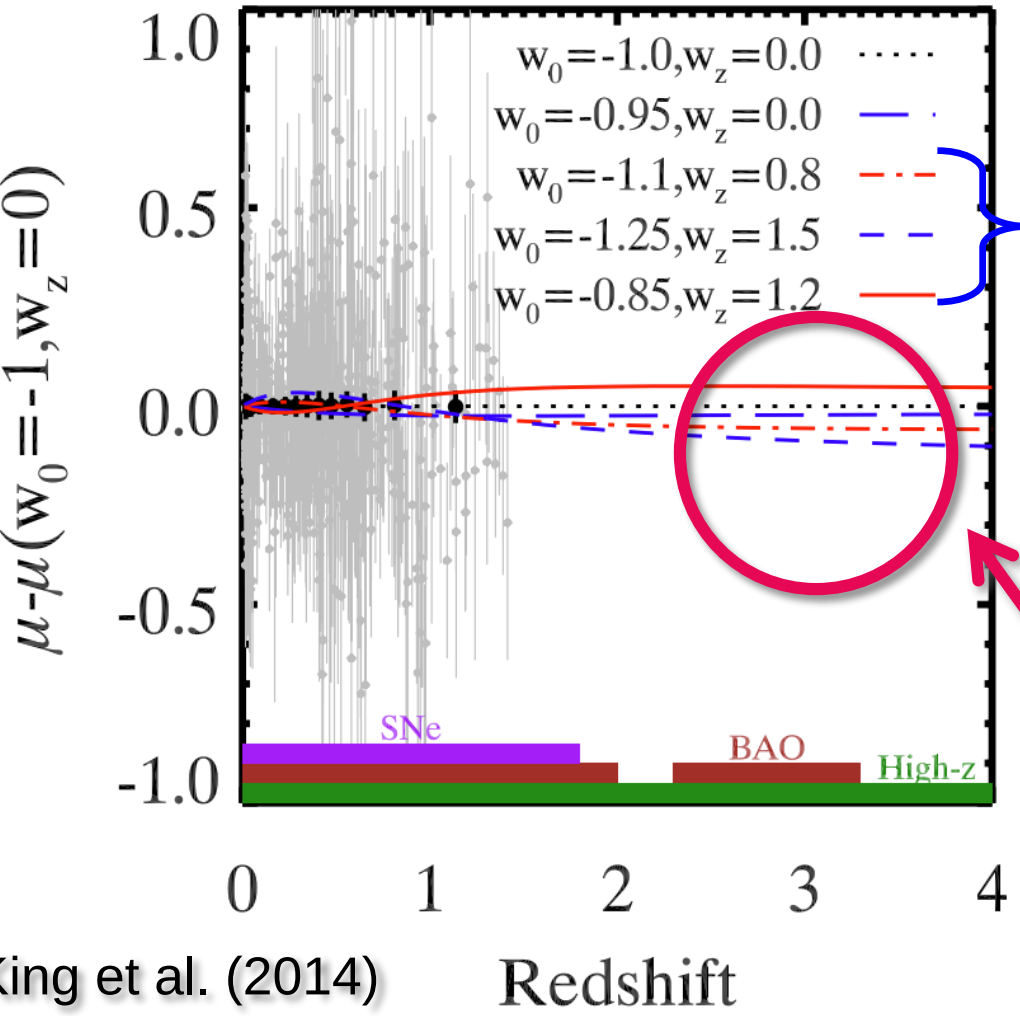

King et al. (2014)

Time variable models

Variability needs a long time span.

⇒We need to probe at high-z.

Figure 1. Hubble diagram showing a distance modulus, μ, normalized to that expected for a ΛCDM universe (dotted black curve). Blue and red curves

Type Ia supernova are less useful at high-z because,

- Too faint to be observed at high-z
- Long time-delay before reaching Chandrasekhar mass (a few Gyrs).
  ⇨Very few at high-z

We need a brighter standard candle.

~~Standard candle~~

Standard campfire

What can be a standard campfire?

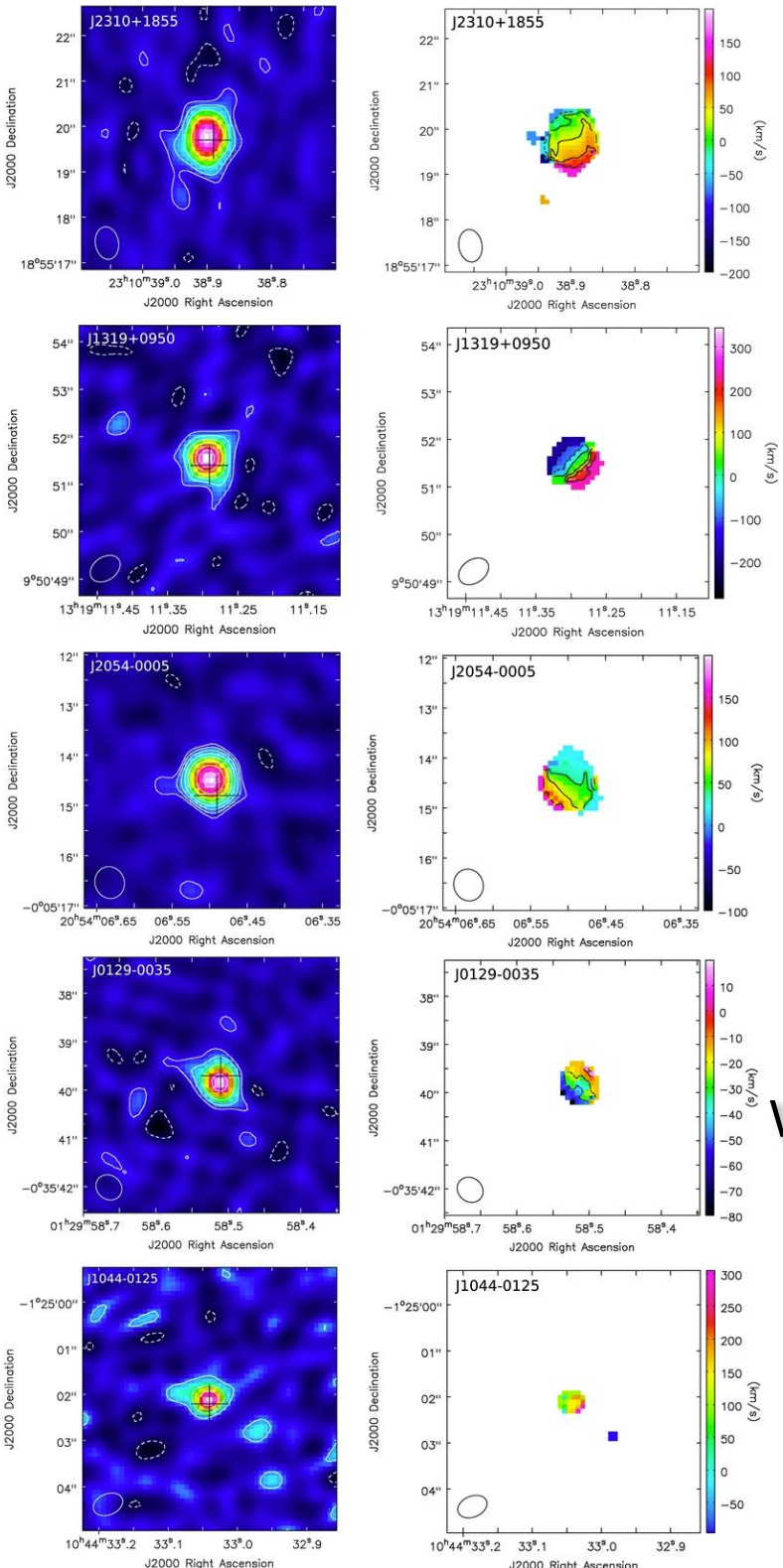

Sub-millimeter galaxies are being observed at high-z with ALMA

Wang et al. (2013)

Table 2
ALMA Observations

Source	t_{on} (min)	$z_{[C\,II]}$	$S\Delta v$ (Jy km s^{-1})	FWHM$_{[C\,II]}$ (km s^{-1})
(1)	(2)	(3)	(4)	(5)
J2310+1855	50	6.0031 ± 0.0002	8.83 ± 0.44	393 ± 21
J1319+0950	80	6.1330 ± 0.0007	4.34 ± 0.60	515 ± 81
J2054−0005	40	6.0391 ± 0.0001	3.37 ± 0.12	243 ± 10
J0129−0035	60	5.7787 ± 0.0001	1.99 ± 0.12	194 ± 12
J1044−0125	87	5.7847 ± 0.0007	1.70 ± 0.30	420 ± 80

Large sample of CO galaxies compiled from literature

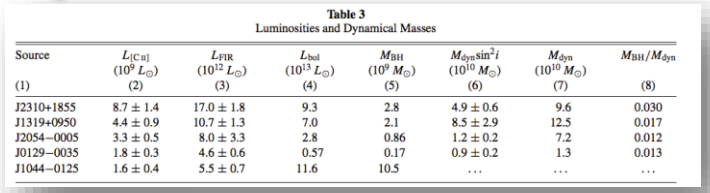

Table 3
Luminosities and Dynamical Masses

Source	$L_{[C\,II]}$ ($10^9\,L_\odot$)	L_{FIR} ($10^{12}\,L_\odot$)	L_{bol} ($10^{13}\,L_\odot$)	M_{BH} ($10^9\,M_\odot$)	$M_{dyn}\sin^2 i$ ($10^{10}\,M_\odot$)	M_{dyn} ($10^{10}\,M_\odot$)	M_{BH}/M_{dyn}
(1)	(2)	(3)	(4)	(5)	(6)	(7)	(8)
J2310+1855	8.7 ± 1.4	17.0 ± 1.8	9.3	2.8	4.9 ± 0.6	9.6	0.030
J1319+0950	4.4 ± 0.9	10.7 ± 1.3	7.0	2.1	8.5 ± 2.9	12.5	0.017
J2054−0005	3.3 ± 0.5	8.0 ± 3.3	2.8	0.86	1.2 ± 0.2	7.2	0.012
J0129−0035	1.8 ± 0.3	4.6 ± 0.6	0.57	0.17	0.9 ± 0.2	1.3	0.013
J1044−0125	1.6 ± 0.4	5.5 ± 0.7	11.6	10.5	…	…	…

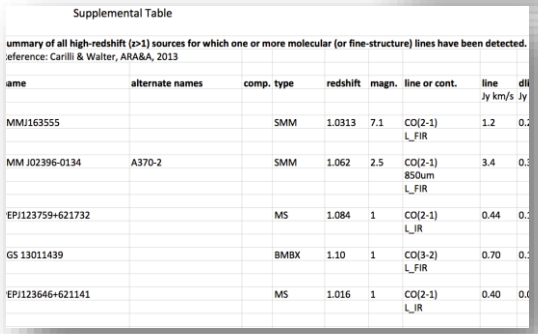

Supplemental Table

ummary of all high-redshift (z>1) sources for which one or more molecular (or fine-structure) lines have been detected.
eference: Carilli & Walter, ARA&A, 2013

ame	alternate names	comp.	type	redshift	magn.	line or cont.	line Jy km/s	dli Jy
MMJ163555			SMM	1.0313	7.1	CO(2-1) L_FIR	1.2	0.2
MM J02396-0134	A370-2		SMM	1.062	2.5	CO(2-1) 850um L_FIR	3.4	0.3
EPJ123759+621732			MS	1.084	1	CO(2-1) L_IR	0.44	0.2
GS 13011439			BMBX	1.10	1	CO(3-2) L_FIR	0.70	0.2
EPJ123646+621141			MS	1.016	1	CO(2-1) L_IR	0.40	0.0

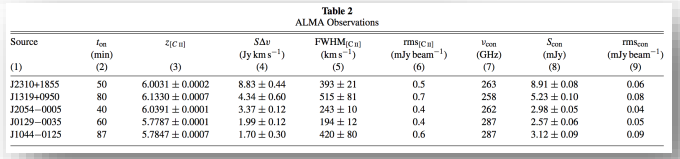

Table 2
ALMA Observations

Source	t_{on} (min)	$z_{[C\,II]}$	$\Delta\Delta v$ (Jy km s^{-1})	FWHM$_{[C\,II]}$ (km s^{-1})	rms$_{[C\,II]}$ (mJy beam^{-1})	ν_{con} (GHz)	S_{con} (mJy)	rms$_{con}$ (mJy beam^{-1})
(1)	(2)	(3)	(4)	(5)	(6)	(7)	(8)	(9)
J2310+1855	50	6.0031 ± 0.0002	8.83 ± 0.44	393 ± 21	0.5	263	8.91 ± 0.08	0.06
J1319+0950	80	6.1330 ± 0.0007	4.34 ± 0.60	515 ± 81	0.7	258	5.23 ± 0.10	0.08
J2054−0005	40	6.0391 ± 0.0001	3.37 ± 0.12	243 ± 10	0.4	262	2.98 ± 0.05	0.04
J0129−0035	60	5.7787 ± 0.0001	1.99 ± 0.12	194 ± 12	0.4	287	2.57 ± 0.06	0.05
J1044−0125	87	5.7847 ± 0.0007	1.70 ± 0.30	420 ± 80	0.6	287	3.12 ± 0.09	0.09

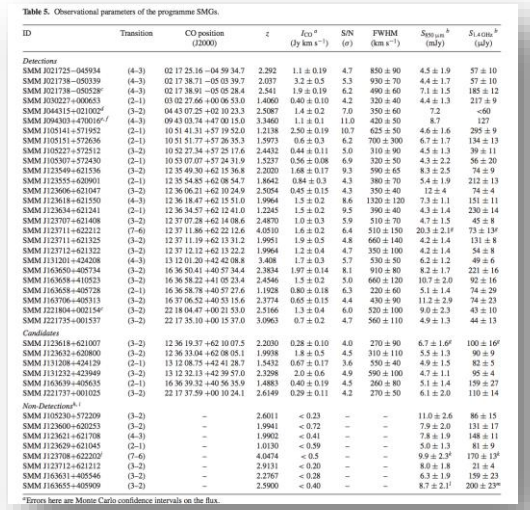

Table 5. Observational parameters of the programme SMGs.

ID	Transition	CO position (J2000)	z	I_{CO} [a] (Jy km s^{-1})	S/N (σ)	FWHM (km s^{-1})	$S_{870\,\mu m}$ [b] (mJy)	$S_{1.4\,GHz}$ [b] (μJy)
Detections								
SMM J021725−045934	(4–3)	02 17 25.16 −04 59 34.7	2.292	1.1 ± 0.19	4.7	850 ± 90	4.5 ± 1.9	57 ± 10
SMM J021738−050339	(4–3)	02 17 38.71 −05 03 39.7	2.037	3.2 ± 0.5	5.3	930 ± 70	4.4 ± 1.7	57 ± 10
SMM J021738−050528[c]	(4–3)	02 17 38.91 −05 05 28.4	2.541	1.9 ± 0.19	6.2	490 ± 60	7.1 ± 1.5	185 ± 12
SMM J030227+000653	(2–1)	03 02 27.66 +00 06 53.0	1.4060	0.40 ± 0.10	4.2	320 ± 40	4.4 ± 1.3	217 ± 9
SMM J044315+021002[d]	(3–2)	04 43 07.25 +02 10 23.3	2.5087	1.4 ± 0.2	7.0	350 ± 60	7.2	<60
SMM J094303+470016[e,f]	(4–3)	09 43 03.74 +47 00 15.0	3.3460	1.1 ± 0.1	11.0	420 ± 50	8.7	127
SMM J105141+571952	(2–1)	10 51 41.31 +57 19 52.0	1.2138	2.50 ± 0.19	10.7	625 ± 50	4.6 ± 1.6	295 ± 9
SMM J105151+572636	(2–1)	10 51 51.77 +57 26 35.3	1.5973	0.6 ± 0.3	6.2	700 ± 300	6.7 ± 1.7	134 ± 13
SMM J105227+572512	(3–2)	10 52 27.34 +57 25 17.6	2.4432	0.44 ± 0.11	5.0	310 ± 90	4.5 ± 1.3	39 ± 11
SMM J105307+572430	(2–1)	10 53 07.07 +57 24 31.9	1.5237	0.56 ± 0.08	6.9	320 ± 50	4.3 ± 2.2	56 ± 20
SMM J123549+621536	(3–2)	12 35 49.30 +62 15 36.8	2.2020	1.68 ± 0.17	9.3	590 ± 65	8.3 ± 2.5	74 ± 9
SMM J123555+620901	(2–1)	12 35 54.85 +62 08 54.7	1.8642	0.84 ± 0.3	4.3	380 ± 70	5.4 ± 1.9	212 ± 13
SMM J123606+621047	(3–2)	12 36 06.21 +62 10 24.9	2.5054	0.45 ± 0.15	4.3	350 ± 40	12 ± 4	74 ± 4
SMM J123618+621550	(4–3)	12 36 18.47 +62 15 51.0	1.9964	1.5 ± 0.2	8.6	1320 ± 120	7.3 ± 1.1	151 ± 11
SMM J123634+621241	(2–1)	12 36 34.57 +62 12 41.0	1.2245	1.5 ± 0.2	9.5	390 ± 40	4.3 ± 1.4	230 ± 14
SMM J123707+621408	(3–2)	12 37 07.28 +62 14 08.6	2.4870	1.0 ± 0.3	5.9	510 ± 70	4.7 ± 1.5	45 ± 8
SMM J123711+622212	(7–6)	12 37 11.86 +62 22 12.6	4.0510	1.6 ± 0.2	6.4	510 ± 150	20.3 ± 2.1[g]	73 ± 13[g]
SMM J123711+621325	(3–2)	12 37 11.19 +62 13 31.2	1.9951	1.9 ± 0.5	4.8	660 ± 140	4.2 ± 1.4	131 ± 8
SMM J123712+621322	(3–2)	12 37 12.12 +62 13 22.2	1.9964	1.2 ± 0.4	4.7	350 ± 100	4.2 ± 1.4	54 ± 8
SMM J131201+424208	(4–3)	13 12 01.20 +42 42 08.8	3.408	1.7 ± 0.3	5.7	530 ± 50	6.2 ± 1.2	49 ± 6
SMM J163650+405734	(3–2)	16 36 50.41 +40 57 34.4	2.3834	1.97 ± 0.14	8.1	910 ± 80	8.2 ± 1.7	221 ± 16
SMM J163658+410523	(3–2)	16 36 58.22 +41 05 23.4	2.4546	1.5 ± 0.2	5.0	660 ± 120	10.7 ± 2.0	92 ± 16
SMM J163658+405728	(2–1)	16 36 58.78 +40 57 27.6	1.1928	0.80 ± 0.18	6.3	220 ± 60	5.1 ± 1.4	74 ± 29
SMM J163706+405313	(3–2)	16 37 06.52 +40 53 15.6	2.3774	0.65 ± 0.15	4.4	430 ± 90	11.2 ± 2.9	74 ± 23
SMM J221804+002154[e]	(3–2)	22 18 04.47 +00 21 53.0	2.5166	1.3 ± 0.4	6.0	520 ± 100	9.0 ± 2.3	43 ± 10
SMM J221735+001537	(3–2)	22 17 35.10 +00 15 37.0	3.0963	0.7 ± 0.2	4.7	560 ± 110	4.9 ± 1.3	44 ± 13
Candidates								
SMM J123618+621007	(3–2)	12 36 19.37 +62 10 07.5	2.2030	0.28 ± 0.10	4.0	270 ± 90	6.7 ± 1.6[g]	100 ± 16[g]
SMM J123632+620800	(3–2)	12 36 33.04 +62 08 05.1	1.9938	1.8 ± 0.5	4.5	310 ± 110	5.5 ± 1.3	90 ± 9
SMM J131208+424129	(2–1)	13 12 08.75 +42 41 28.7	1.5432	0.67 ± 0.17	3.6	550 ± 40	4.9 ± 1.5	82 ± 5
SMM J131232+423949	(3–2)	13 12 32.13 +42 39 57.0	2.3298	2.0 ± 0.6	4.9	590 ± 100	4.7 ± 1.1	95 ± 4
SMM J163639+405635	(2–1)	16 36 39.32 +40 56 35.9	1.4883	0.40 ± 0.19	4.5	260 ± 80	5.1 ± 1.4	159 ± 27
SMM J221737+001025	(3–2)	22 17 37.59 +00 10 24.1	2.6149	0.29 ± 0.11	4.2	270 ± 50	6.1 ± 2.0	110 ± 14
Non-Detections[h,i]								
SMM J105230+572209	(3–2)	–	2.6011	< 0.23	–	–	11.0 ± 2.6	86 ± 15
SMM J123600+620253	(3–2)	–	1.9941	< 0.72	–	–	7.9 ± 2.0	131 ± 17
SMM J123621+621708	(4–3)	–	1.9902	< 0.41	–	–	7.8 ± 1.9	148 ± 11
SMM J123629+621045	(2–1)	–	1.0130	< 0.59	–	–	5.0 ± 1.3	81 ± 9
SMM J123708+622020	(7–6)	–	4.0474	< 0.5	–	–	9.9 ± 2.3[g]	170 ± 13[g]
SMM J123712+621212	(3–2)	–	2.9131	< 0.20	–	–	8.0 ± 1.8	21 ± 4
SMM J163631+405546	(3–2)	–	2.2767	< 0.28	–	–	6.3 ± 1.9	159 ± 23
SMM J163655+405909	(3–2)	–	2.5900	< 0.40	–	–	8.7 ± 2.1[j]	200 ± 23[w]

[a]Errors here are Monte Carlo confidence intervals on the flux.

Bothwell, et al. 2013, MNRAS,429, 3047
Carilli & Walter, 2013, ARA&A, 51, 105
Harris, et al. 2012, ApJ, 752,152
…

195 CO galaxies (z>2), the largest sample

We confirmed *L'CO*-FWHM correlation

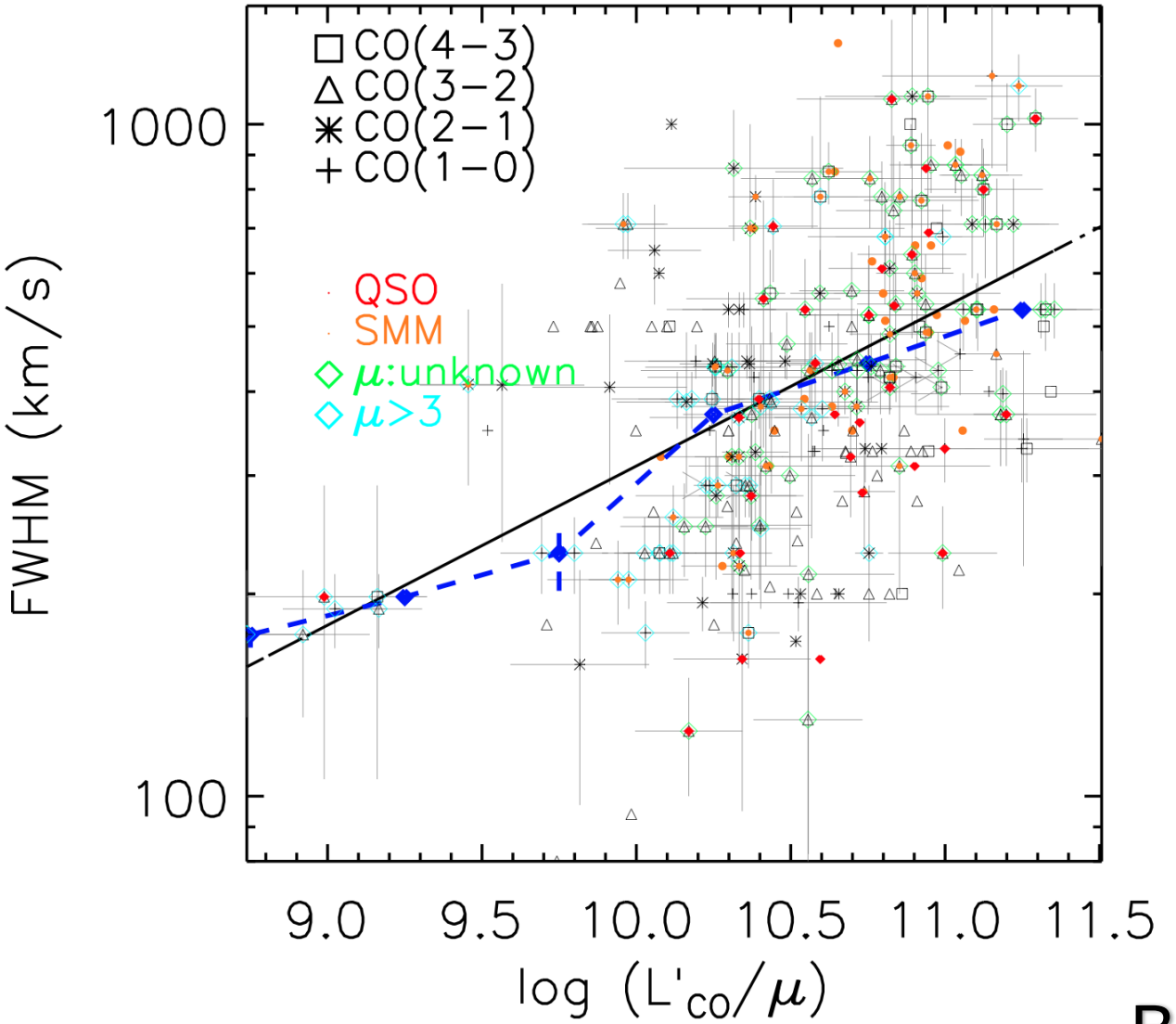

Bothwell, et al. 2013
Harris, et al. 2012

L'_{CO}-FWHM correlation

weak but very significant

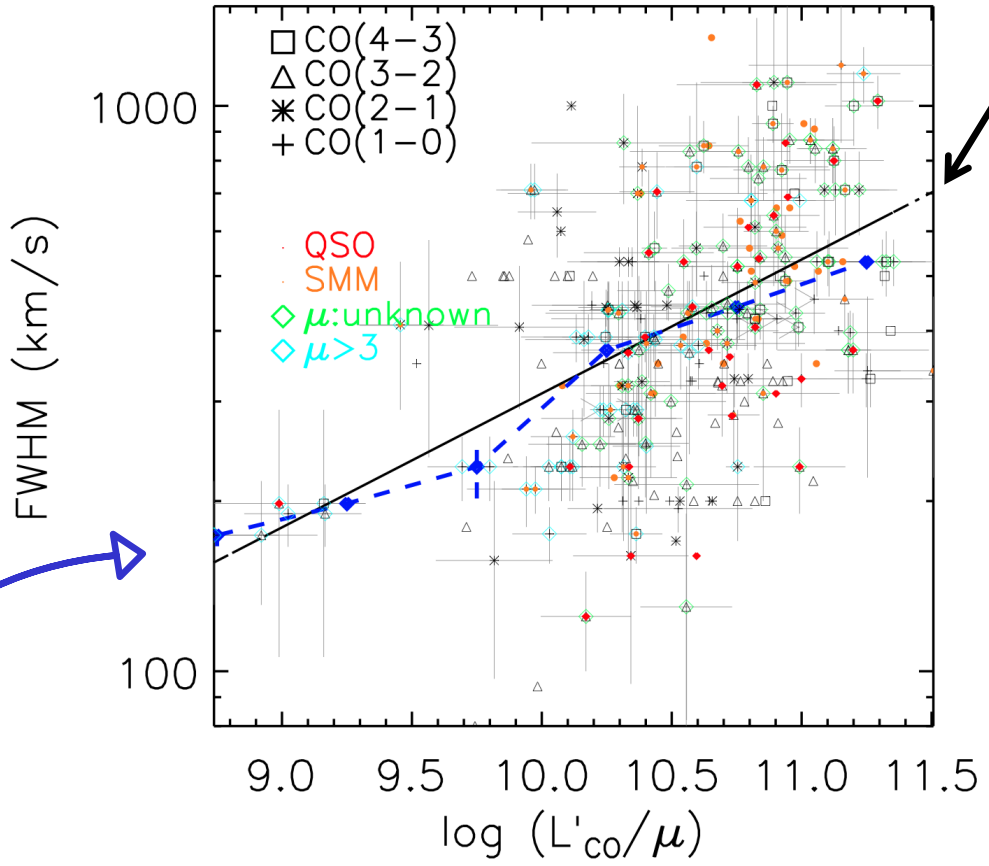

Best-fit power-law:

$$(FWHM) = (0.24 \pm 0.03) \times \log(L'_{CO}/\mu) + (0.12 \pm 0.28)$$

A positive slope @ 8.7σ

Spearman's coeff.	p-value
0.55	1.7e-16

Connecting median

43% of scatter, consistent with thin random disk (~45%).

Not surprising. At low-z, well-known Tully-Fisher relation exists.

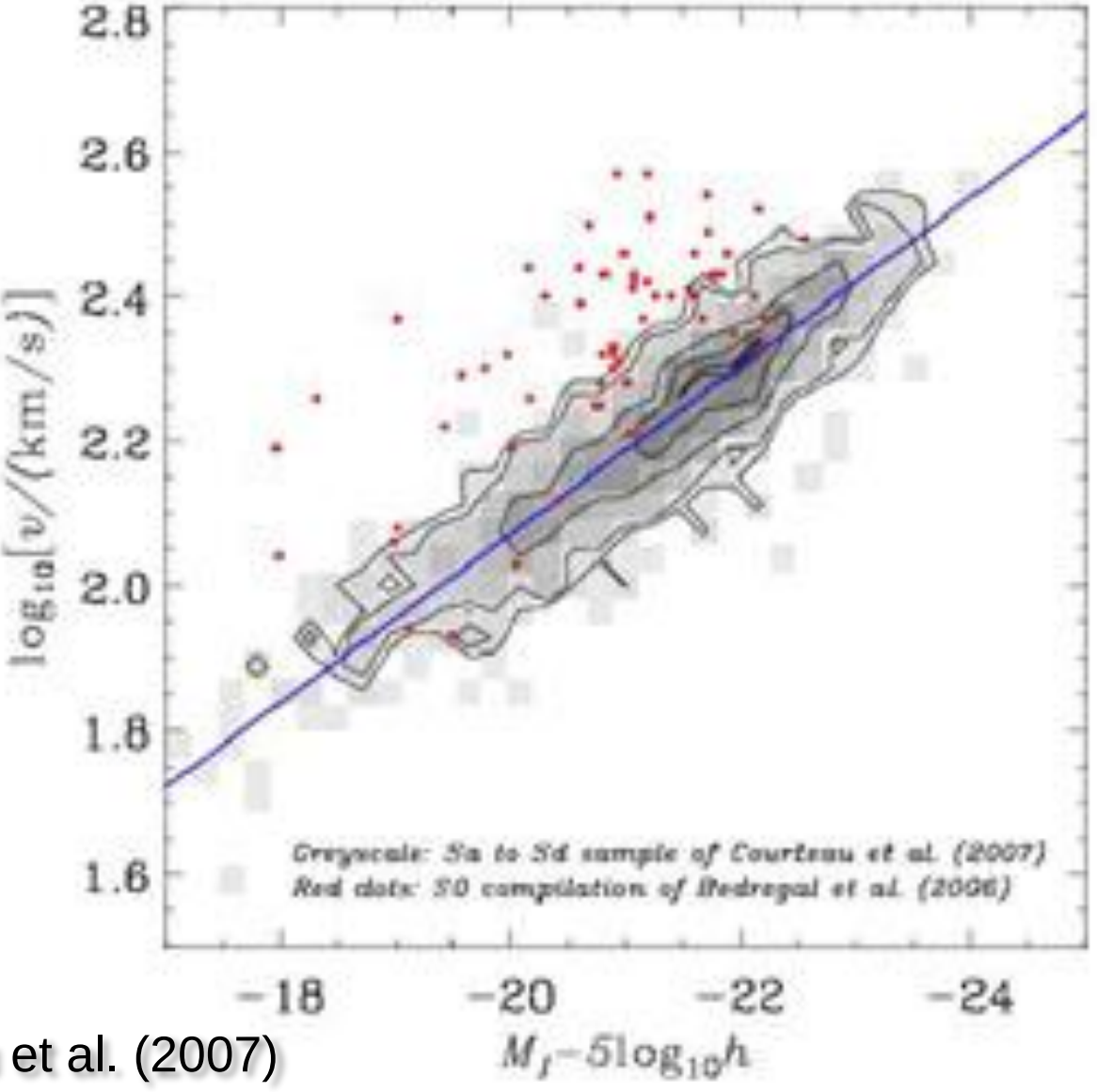

Courteau et al. (2007)

L'CO-FWHM correlation can be considered high-z version of Tully-Fisher relation

No sign of z evolution

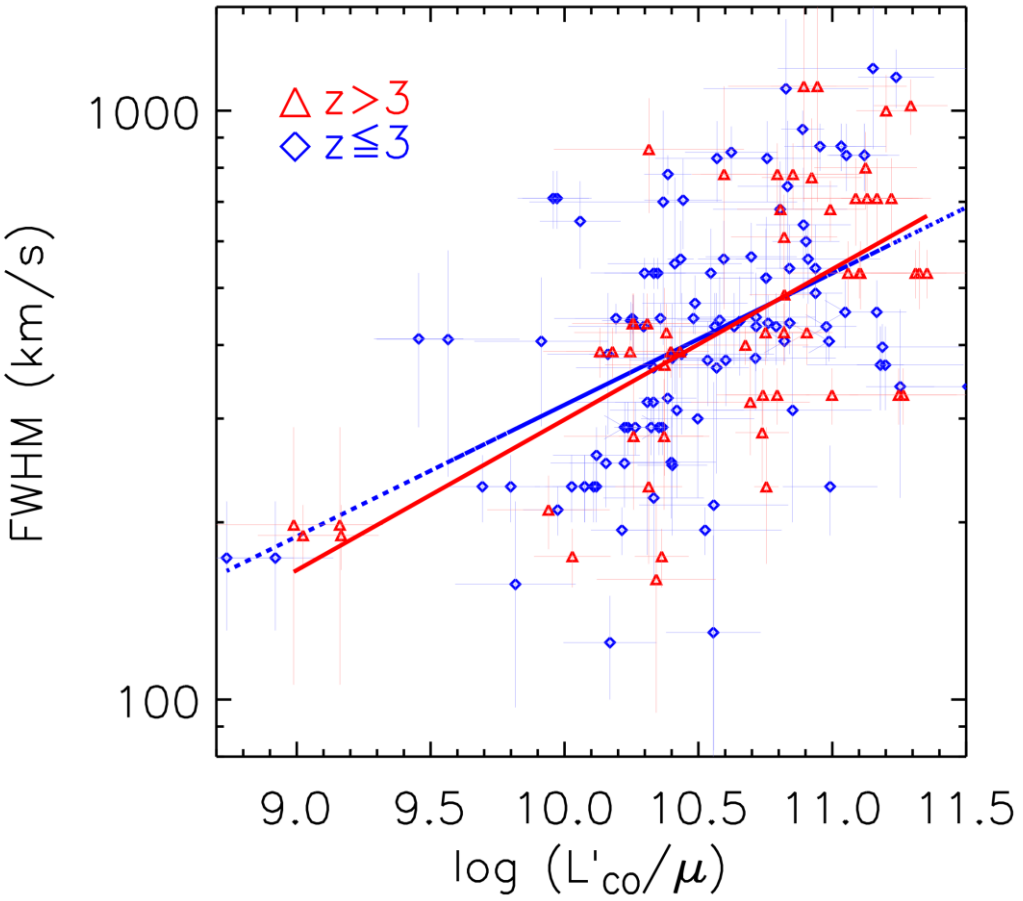

Best-fit power-laws are:

FWHM (km/s) $\propto (L'/\mu)^{0.22\pm0.04}$ (z≤3, blue)

FWHM (km/s) $\propto (L'/\mu)^{0.25\pm0.04}$ (z>3, red)

⇒ Consistent to each other.

Hubble diagram to z~6

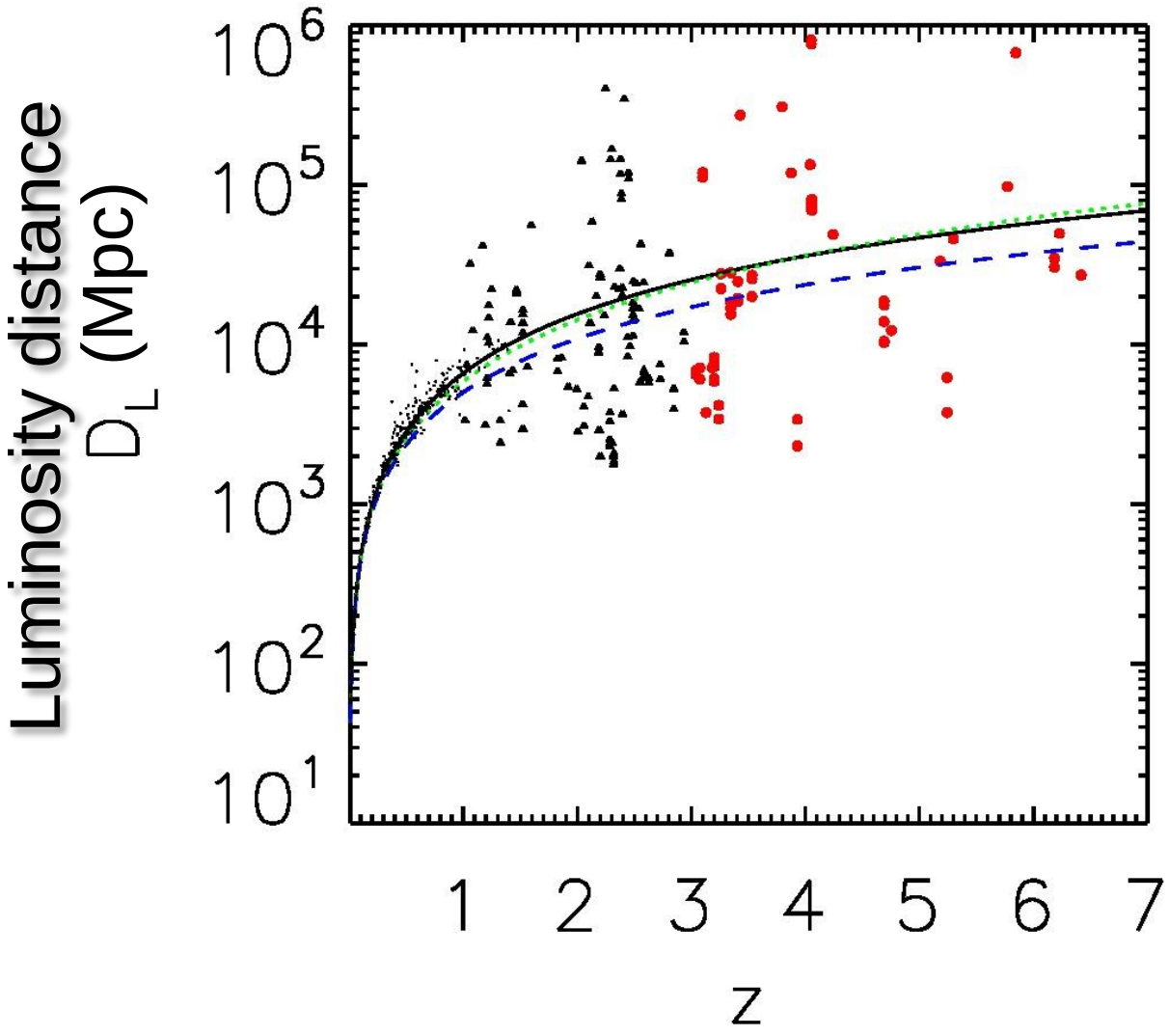

black solid:(Ω_M,Ω_Λ)=(0.3,0.7)
green dotted: (Ω_M , Ω_Λ)=(0.3,0.0)
blue-dashed:(Ω_M , Ω_Λ)=(1.0,0.0)

For now, errors are too large to conclude. However…

ALMA will improve,

- Number of objects will improve significantly
  - Cont. of S1.1mm = 3 mJy (z = 6.5) in 2.5sec
  - Statistics to beat random noise.

- Inclination & Magnification measurements
  - ALMA spatial resolution ~0.037” (110 GHz)
    ~0.2 kpc at z=6.
  - Sufficient to resolve submm galaxies (several kpc)

Summary

- The largest sample of submm galaxies with CO detection at z>2 (*N*=195)
- A weak but very significant
  L'CO-FWHM correlation
- Possibly used for a Hubble diagram to z~6 and beyond.
- *Goto & Toft, A&A, 579 (2015) A17*